Applied Thermal Engineering 246 (2024) 122943

Contents lists available at ScienceDirect

Applied Thermal Engineering

journal homepage: www.elsevier.com/locate/ate

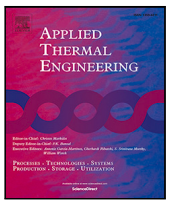

Experimental characterization of an industrial burner operated with simulated EGR

S. Galeotti [a,*], A. Picchi [a], R. Becchi [a], R. Meloni [b], G. Babazzi [b], C. Romano [b], A. Andreini [a]

[a] Department of Industrial Engineering, University of Florence, Italy
[b] Baker Hughes, Via F. Matteucci 2, Florence, Italy

ARTICLE INFO

Keywords:
Gas turbine
Emissions
Combustion diagnostic
EGR

ABSTRACT

The implementation of Exhaust Gas Recirculation (EGR) in gas turbines can become an interesting opportunity to enhance the coupling between natural gas fueled GT power plants and Carbon Capture and Storage (CCS) systems. In fact, as the CO_2 content of the incoming flow increases, performance of CCS units improves in terms of efficiency and compactness. As a drawback, the oxygen content available for the combustion reaction decreases, making the combustion process challenging in terms of flame stability and therefore engine operability. This work presents the results of an experimental campaign investigating the behavior of an industrial burner operated with simulated EGR. For the investigation EGR is recreated by diluting standard air with CO_2. The burner is operated at ambient pressure in a single sector optical test rig with tubular quartz liner, using natural gas as fuel. The effect of fuel split between premix and pilot line was investigated along with the lack of oxygen caused by EGR. OH* chemiluminescence imaging was employed to study flame topology, and exhaust gas analysis was performed. Emission measurements showed significant NO_x reduction, but at the same time as expected CO levels increased remarkably under EGR-like conditions. Additionally, CO_2 addition is found to trigger thermoacoustic instabilities in certain conditions, limiting the EGR operability window.

1. Introduction

As the global community strives to meet climate targets and reduce the adverse effects of greenhouse gas emissions, the need for innovative and effective solutions to mitigate carbon dioxide (CO_2) impact has become paramount. Despite the emerging renewable sources, the employment of natural gas in the energy sector is expected to increase because of its great flexibility [1]. The development and adoption of innovative technologies like Carbon Capture and Storage (CCS) systems integrated with gas turbines power plants have the potential to play a pivotal role in achieving these emission reduction targets.

The efficiency of CCS systems grows with the CO_2 concentration of the turbine exhaust, which can be increased with Exhaust Gas Recirculation (EGR) [2,3], in order to make the process more cost-effective. EGR is a well-established technique in internal combustion engines to limit NO_x emissions thanks to flame temperature reduction. On the other hand, the application of EGR in Gas Turbine engines has not yet found a practical utilization due to its expensive and complex installation, and the associated emission reduction can already be achieved by modern Dry Low NOx (DLN) combustion technologies, which are usually able to provide close to single digit emissions [4]. EGR becomes an interesting option in GT engines considering the possibility to improve the efficiency of CCS units by increasing the CO_2 content of the exhaust gases. As a drawback, the decrease in oxygen content of the combustion air is extremely challenging in terms of combustion stability. The effect of EGR at engine conditions has been investigated in the past, showing that CO and UHC emissions significantly increase, therefore limiting the achievable EGR level [5]. The same study reported also that EGR was found to have a beneficial effect on the damping of thermoacoustic instabilities. Recent works confirm the results relative to CO emission increase [6], while the effect of EGR on the flame dynamic behavior is not univocal. A recent study [7] showed that the dynamic flame response is altered not only by the lack of oxygen, but at very low oxygen levels the chemical composition of the oxidizer has also an effect.

The present work fits in this context with the purpose of contributing to the development of new burner concepts, able to efficiently operate in unconventional operating conditions such as exhaust gas recirculation. An experimental campaign was performed at ambient pressure on a burner designed to operate in standard conditions without EGR, in order to identify critical issues and limitations of the current technologies.

* Corresponding author.
E-mail address: sofia.galeotti@unifi.it (S. Galeotti).

https://doi.org/10.1016/j.applthermaleng.2024.122943
Received 2 November 2023; Received in revised form 4 March 2024; Accepted 12 March 2024
Available online 15 March 2024

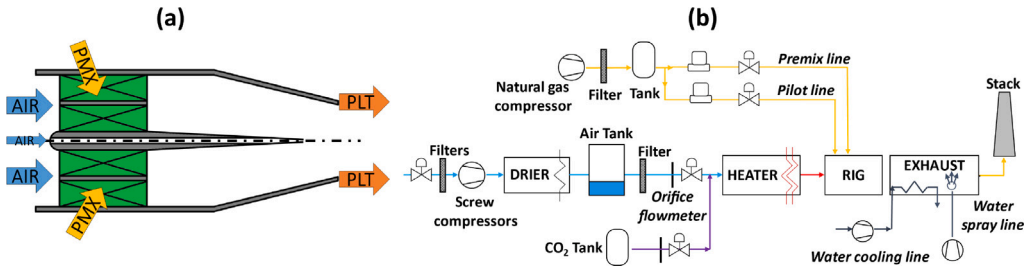

Fig. 1. Investigated burner schematic (a) and combustion test cell plant (b).

Recreating real EGR conditions at lab scale is quite challenging because of the associated costs and plant complications. The present work is the first step of a more general screening, with the purpose of studying different burners and various solutions to improve flame stability, to be compared under the same conditions. CO_2 addition in the airflow feeding the burner has been chosen to reproduce EGR conditions, because it offers the opportunity to manage storage better than mixtures with nitrogen, while preserving the purpose of the investigation.

The burner was fueled with natural gas and operated in a single sector optical test rig with tubular liner. Different conditions have been tested, varying the inlet oxygen level and the fuel split between pilot and premixed lines, in order to investigate the effect of these parameters on the combustion process. Flame topology was studied with OH* chemiluminescence imaging and emission levels of CO and NO_x were measured with exhaust gas analysis. High frequency OH* chemiluminescence and dynamic pressure sensors have been also employed to monitor the dynamic behavior of the flame, which has been found to vary with CO_2 addition.

This test campaign is part of the European project TRANSITION (fuTure hydRogen Assisted gas turbiNeS for effective carbon capTure IntegratiON) which has the purpose of developing advanced combustion technologies for natural gas fired gas turbines to permit engine operations with high EGR rates, with a consequent drastic reduction of the CCS costs and units' size [8]. Ambient pressure tests with single sector test rig can be considered as the first step of an optimization process to be placed in the more general project work frame.

2. Test rig and operating conditions

2.1. Burner description

The investigated burner is a lean premixed burner developed by Baker Hughes for industrial gas turbine applications. A thorough description of the burner geometry and its design can be found in [9–12].

Fig. 1a shows a schematic of the burner cross-section. It is composed by two counter-rotating axial swirlers and a center body with an air purge. Two independent fuel lines are present: the pilot line (PLT) injects the fuel directly in the combustor chamber through circumferentially equally spaced holes, helping the flame stabilization. The premixed line (PMX) delivers the fuel at the tip of the inner swirler, so that it mixes with the airflow thanks to the strong turbulence created by the shear layer generated between the two swirlers [12].

2.2. Test rig configuration

The burner was investigated in the reactive test cell of the THT Lab of the University of Florence, whose schematic layout is outlined in Fig. 1b. The same test cell has been exploited in the past for investigations on novel low NO_x burners for heavy duty gas turbines [13,14].

Compressed air is supplied with a mass-flow up to 1 kg/s at 10 barA by two screw compressors with built-in modulating valve to keep the delivery pressure constant; The compressed air flows through several filters and a dryer (dew point −20 °C) before entering into the test cell. An electric heater (600 kW) is used to heat the airflow, and the inlet temperature is kept constant by modulating the power input with a proportional integral derivative system. The air mass flow rate is controlled with a globe valve located upstream of the heater, and a high-temperature control disk valve is installed downstream of the rig to set the operating pressure. A water jacket exhaust duct with straight circular cross-section (about 1 m length) is placed between the rig and the stack, to avoid effects of the backpressure valve on the combustion processes. Inside the water jacket duct, four water sprayers are used to quench the exhaust and keep the temperature inside the valve operating range. The mainstream mass flow rate is measured with calibrated orifice flow-meters (standard EN ISO 5167-1), with an error of 1% according to the Kline and McClintock method [15].

CO_2 used to simulate EGR conditions is stored in a pressurized tank and injected in the main air flow line upstream of the electric heater, in order to deliver to the test section a homogeneous mixture, both in terms of temperature and composition. Regarding the fuel lines, natural gas is taken from the local gas network (20 mbar) and compressed to 16 bar. The screw compressor is equipped with several filters (micron rating up to 0.1) to remove contaminants from the gas flow, and a 200 liters tank is installed on the delivery line to smooth out pressure fluctuations. A total flow rate of maximum 90 Nm^3/h can be delivered with the two fuel lines serving the test cell. Mass flow rates are controlled with globe valves and measured with dedicated mass flow meters. Shut off valves are also installed along the lines for safety reasons. Natural gas supply on the domestic line varies throughout the day, and for this reason fuel composition is analyzed after each test.

The test article is designed to allow optical measurements of the flame region. Fig. 2a shows a picture of the test rig, and the cross-section is shown in Fig. 2b. The external casing consists of an upstream vessel, through which the burner enters the test article, and a downstream vessel, equipped with two perpendicular optical windows for flame visualization. The combustor is made of a 2.5 mm thick cylindrical quartz liner, held in place thanks to a blocking system made of four tie rods and four springs that connect the dome to the following duct, used to convey the exhaust gases toward the test rig exhaust system. The quartz cylinder is approximately 2.5 diameters long, to ensure a complete flame development for a proper flame visualization. The flame tube is cooled by forced convection of a fraction of the incoming air that flows in the annulus between the liner and the confining vessel, not used in the combustion process. The dome plate is cooled through a series of inclined effusion holes. Dedicated flow checks were performed to evaluate the flowsplit between liner and dome cooling and the combustion air. A spark plug is used for ignition, and it is located along the flame tube downstream of the optical liner. An in-depth description of the test rig design can be found in [16].

2.3. Operating conditions

The experimental campaign has been performed at ambient pressure with natural gas as fuel. The purpose of the present work is to characterize the burner behavior under conditions that recreate the lack of

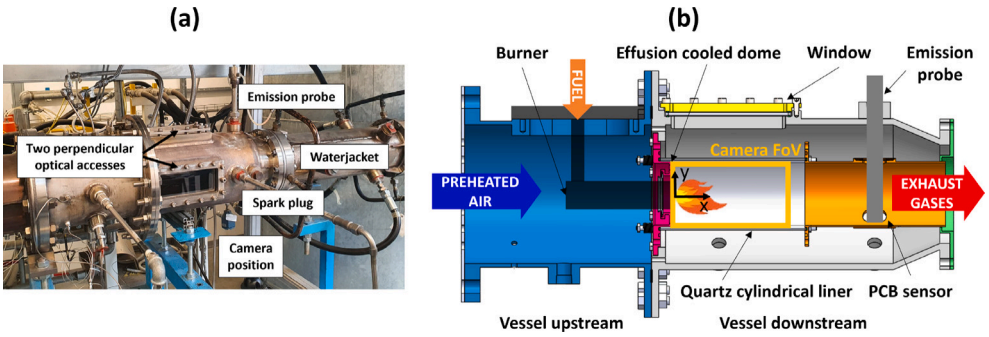

Fig. 2. Reactive test rig picture (a) and test article cross-section (b) at the THT Lab of the University of Florence.

Table 1
Burner operating conditions.

Inlet temperature	T_{inlet}	300	[°C]
Burner pressure drop	$\Delta P/P$	4.2	[%]
Adiabatic flame temperature	T_{flame}	Constant	[–]
Fuel split	PMX%	0–80	[%]
Inlet oxygen molar fraction	x_{O2}	21–17	[%mol]

oxygen caused by EGR. As anticipated EGR-like conditions have been reproduced by diluting the airflow entering the test rig with CO_2.

EGR condition is here represented by the inlet oxygen molar fraction x_{O2}, which is a key similarity parameter between real EGR and simulated conditions. In real EGR the oxidizer composition depends both on the fraction of the recirculated exhaust and on the equivalence ratio of the combustion process, which varies with the engine load. In order to scale this last effect and show a truthful comparison, all the presented results have been obtained at the same adiabatic flame temperature, evaluated assuming a perfect mixing between the burner combustion air and the total amount of fuel injected. Inlet oxygen content has been varied to simulate different EGR levels, adjusting the fuel flow to match the target adiabatic flame temperature. The air mass flow rate was also varied to maintain the right burner pressure drop depending on the added CO_2. Oxidizer inlet temperature and burner pressure drop have been kept constant during the entire test campaign at 300 °C and 4.2% respectively. The ratio of fuel flow injected with the premix line and total fuel flow rate is denoted as PMX[%]. The tested operating points are summarized in Table 1. The fuel split has been varied in order to study the combined effect of this parameter with the oxygen depletion due to EGR. The premix fuel line was not fed further to not exceed the 80%PMX fuel split configuration. This limitation is due to the occurrence of thermoacoustic instabilities that arise when the burner is operated in the present test rig with tubular liner when the premix fuel fraction exceeds this value. Furthermore, since the optical test rig has a quartz liner, vibration levels that are normally tolerable when the burner is operated inside the standard combustion chamber, are not allowable during the tests.

2.4. Experimental methods

Concerning the rig instrumentation, the test article is equipped with various thermocouples and static pressure ports to monitor the flow conditions. An emission probe is employed to analyze the exhaust composition through a HORIBA PG350. The probe is made of several radially spaced holes, and it is plunged into the flame tube to extract the exhaust gases, as shown in Fig. 2b. After being extracted, the gases flow through a thermally insulated pipeline kept at 150 °C, are dried by a HORIBA PSS-5H refrigerator and finally reach the gas analyzer. The gas analyzer is properly calibrated right before each test employing a rack of calibrated gas mixture tanks. Chemical species measured by the gas analyzer are O_2, CO_2, CO and NO_x, but only the results relative to CO and NO_x will be presented. O_2 and CO_2 levels were monitored during tests to ensure the right operating conditions and to correct emission values, as explained in Section 3.2.

A dynamic pressure sensor (PCB) is also installed on the test rig to monitor pressure oscillations, with an acquisition frequency of 12.8 kHz. The probe is located along the flame tube downstream of the optical liner, at the same axial location of the emission probe, about 350 mm downstream of the burner exit.

Chemiluminescence of the OH* radical was employed to detect the reaction zone and its position in various operating conditions. For OH* chemiluminescence measurements a high-speed camera (Phantom M340) was coupled with the Hamamatsu image intensifier through a relay lens. In addition, a UV lens and bandpass filter (CWL = 310 +/−5 nm) were mounted on the image intensifier to be able to capture the OH* transition, which has its peak emission intensity in the UV spectrum at around 310 nm. Images were acquired at 1000 Hz with a 0.5 ms intensifier gate.

Image post processing was performed with Matlab© with user-defined routines. After background subtraction and spatial calibration, images are averaged over time, in order to study the flame steady structure. Chemiluminescence is a line-of-sight technique, meaning that the emission intensity collected by the camera is given by the signal integrated along the ideal line that connects the camera sensor to the desired field of view. The flame shape on the mid-plane can be reconstructed through the application of an inverse Abel transformation, for which a detailed description can be found in [17]. Briefly, ignoring the flame self-absorption contribution and assuming an axial symmetry of the image, the OH* intensity distribution on the burner mid-plane can be retrieved. To match the symmetry requirement Abel deconvolution has been applied only on time averaged images, but as the results will show, pilot fuel is injected with discrete jets, and therefore it is not properly correct to assume axial symmetry. For a first evaluation, however, it was considered useful for the investigation to also examine the Abel deconvoluted images, since they bring additional information to line-of-sight images.

For the analysis of the flame dynamic behavior Proper Orthogonal Decomposition (POD) of high speed OH* chemiluminescence images was performed. POD analysis is able to identify modal coherent structures and energetic modes of the flame, converting time-dependant data into orthogonal modes ordered with decreasing energy. Since this is not the main focus of the investigation, the in-depth description of the mathematical procedure is not reported, and more details can be found in [18–20]. In summary, POD applied to OH* chemiluminescence images provides three quantities to describe the flame structure: eigenvalues, eigenvectors, and the POD modes. The POD modes constitute an orthogonal basis, extracted decoupling the spatial and temporal contributions, determining the most energetic structures. Eigenvalues represent the energy contribution of each mode to the reconstruction of the reaction zone, while eigenvectors retain the temporal information related to each mode.

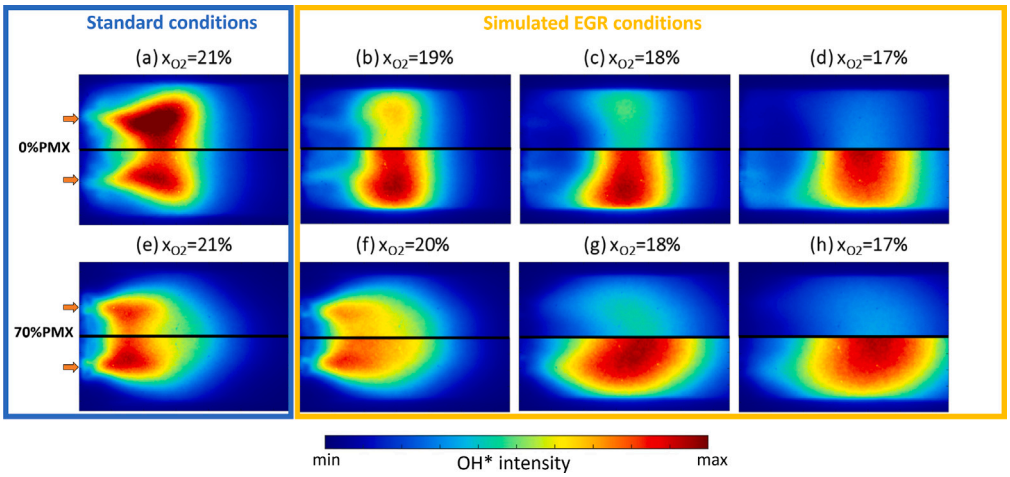

Fig. 3. Time-averaged OH* chemiluminescence images at Tflame = constant for 0%PMX (a-b-c-d) and 70%PMX (e-f-g-h). (Upper halves: absolute OH* intensity, lower halves: normalized with each own maximum).

3. Results and discussion

The aim of the present work is to understand the potential design modification needed to operate stably in an oxygen depleted environment caused by EGR. With respect to standard conditions (x_{O2} = 21%) CO_2 content was increased to lower the oxygen available for the combustion process up to x_{O2} = 17%. Different splits between pilot and premixed fuel lines have been explored, keeping the adiabatic flame temperature constant, as reported in Table 1.

OH* chemiluminescence images will be shown first to highlight the different flame structures, pointing out the key role of pilot fuel jets in flame stabilization. Afterwards emission measures will be shown, since the increase of CO levels is a critical aspect with high EGR rate, while a beneficial effect is expected on NO_x. Lastly the dynamic behavior of the flame will be presented, investigated both with pressure sensors and OH* imaging, with very interesting results.

3.1. OH* chemiluminescence results

Time averaged maps of OH* intensity are presented in Fig. 3 with decreasing inlet oxygen content going from left to right.

Only two different fuel splits are reported as they are sufficient to describe the variation of flame topology: a fully diffusive split (0%PMX) and a representative condition for higher premixing level (70%PMX). Intermediate fuel split conditions have been omitted since they do not provide additional information. The camera field of view (FoV) is illustrated in Fig. 2b, together with the coordinate system centered on the burner outlet. For clarity the position of pilot fuel injection is reported with arrows on the OH* maps relative to standard conditions.

The upper halves of the images show OH* absolute intensity, while in the lower halves OH* intensity is normalized with the maximum value of each case. Since all the presented results have been obtained with the same intensifier set-up, it is possible to compare the absolute OH* intensity between different conditions.

Considering at first the results with standard air (Fig. 3a and e), fuel split significantly affects the flame shape. With higher fraction of fuel injected with the premixed line the flame closes toward the centerline, and the absolute OH* intensity decreases. The pilot jets are clearly distinguishable near the burner exit for both the fully diffusive case (a) and the more premixed one (e). For a better understanding, Fig. 4 shows the Abel deconvolution of OH* chemiluminescence for these two cases: even when the fuel split is more premixed the flame still anchors in correspondence of the pilot jets, which seem to give the greatest contribution to the reaction zone, resulting in a predominantly diffusive flame. The effect of the premixed line is to take the flame closer to the burner exit and widen the reaction zone radially toward the burner axis. Additionally, with higher premixing the maximum OH* intensity decreases, which means lower local heat release [21]. The lower temperature peak has a beneficial effect on NO_x emission, as it will be detailed in the next section.

Looking at the effect of simulated EGR it is evident that the absolute OH* intensity significantly decreases when inlet oxygen decreases, for both fuel splits. Line-of-sight absolute OH* intensity averaged over the whole measurement area is reported in Fig. 5a for both fuel splits as a function of the inlet oxygen content, as an indication of the global reactivity. In standard conditions (x_{O2} = 21%) averaged OH* value is significantly higher for the fully diffusive case (0%PMX), but reducing the inlet oxygen level this difference becomes marginal. The fully piloted case has a linear decrease, while with higher premixing lower maximum values are first balanced by the increase in the extension of the reaction zone (Fig. 3e and f). With further reduction of the inlet oxygen level averaged OH* values decrease, with a lower profile slope than the fully diffusive case.

Lowering the inlet oxygen content has also the additional effect of shifting the reaction zone downstream from the burner exit and making it more diffuse. The oxygen content depletion leads to a slowdown of the reaction process, as shown in several studies where laminar flame velocity decreases with CO_2 dilution [22,23]. Indeed, the reaction zone becomes more widespread, moving toward diffuse combustion regimes and reaching an extension that almost covers the entire combustion chamber (Fig. 3c-d-g-h). The same behavior has also been encountered in a previous work from the authors, where a similar analysis was conducted on a different burner [24].

In order to quantify the flame lift-off and elongation, Fig. 5b reports the axial position of the maximum of OH* intensity averaged over the radial coordinate *y* for the Abel deconvoluted images. Values have been scaled with the minimum one, which corresponds to the case with higher premixing and without CO_2 addition. As shown by Fig. 4, in standard conditions with higher premixed fuel fraction the flame is closer to the burner exit. This trend is reversed with CO_2 addition, as the diffusive case is less affected by the decrease in laminar flame speed caused by lower oxygen levels, thanks to locally richer conditions. The overall increase going from standard conditions to the lower oxygen level in the distance of the main reaction zone from the burner exit is almost 3 times higher for the more premixed case. Therefore, when the burner is operated within the gas turbine conventional combustion chamber designed to operate without exhaust gas recirculation, the increase in flame length due to high EGR levels could be partially compensated using higher piloted fuel splits (lower %PMX). At high pressure the flame length decreases significantly [4] but although this

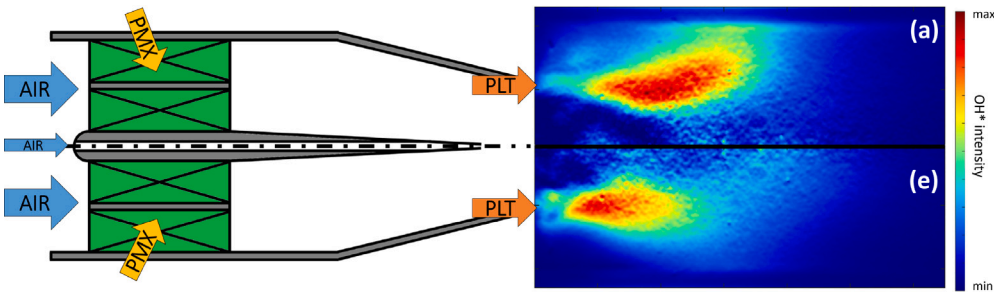

Fig. 4. Abel deconvolution of time-averaged OH* chemiluminescence images (not normalized) at Tflame = constant for 0%PMX (a) and 70%PMX (e).

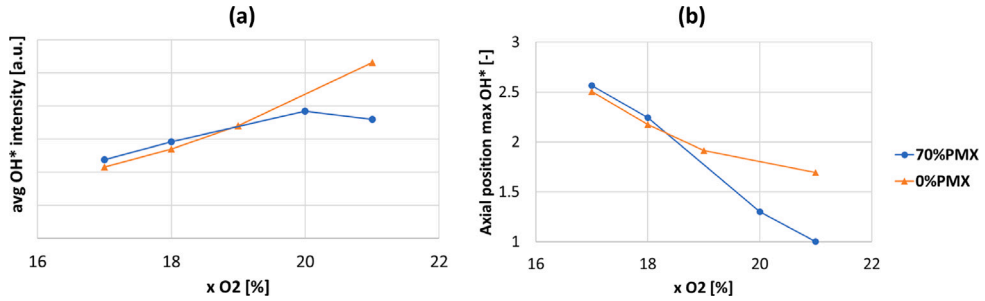

Fig. 5. Averaged OH* intensity (a) and reaction zone lift-off (b) for 0 and 70%PMX with constant adiabatic flame temperature and decreasing inlet oxygen content.

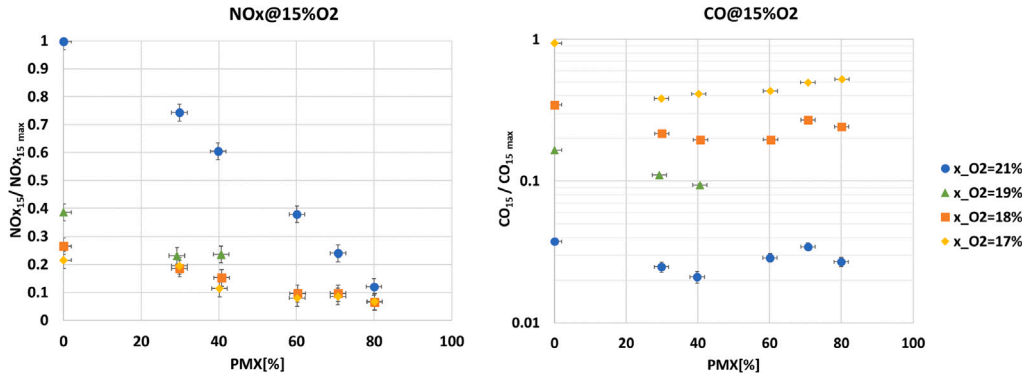

Fig. 6. Normalized NO_x and CO emission measurements at Tflame = constant.

phenomenon has been observed at ambient pressure, this result still provides a useful indication of flame behavior under EGR conditions, and should be taken into account for burner design optimization.

3.2. Emission measurement results

Fig. 6 shows the results of NO_x and CO emission measurements, which have been corrected with the following expression in order to take into account the lower inlet oxygen content [5] (same for CO).

$$NO^*_{x\,15} = NO_{x\,dry} \cdot \frac{0.2095 - 0.15}{2 - 0.2095} \frac{2 - x_{O2\,inlet}}{x_{O2\,inlet} - x_{O2\,dry}} \quad (1)$$

Starting with the results without EGR (blue symbols), NO_x emissions decrease with an almost linear trend with increasing premixed fuel fraction. Even though OH* chemiluminescence images showed that the flame still stabilizes in correspondence of the pilot jets (Fig. 4), the higher premixing level avoids hot richer spots where NO_x are formed. Indeed OH* absolute intensity is lower with lower pilot fraction.

The effect of fuel split on CO emissions with standard air as oxidizer is less evident and non-monotonic. The overall equivalence ratio is lean for all the tested configurations, but as recalled before the diffusive pilot flames give rise to locally rich conditions, where CO oxidation is not completed. Increasing the premixed fuel fraction CO emissions are slightly lower because of the enhanced mixing, until they rise again. This last condition corresponds to OH* image of Fig. 4e, where the flame is still anchored in correspondence of the pilot jets. Near the burner axis, where the premixed fuel mixture is present, OH* intensity is quite low, and these high CO emissions suggest that the combustion of the premixed fuel is not completed. With further increase in the premix fuel fraction (80%PMX) CO decreases again, as the premixed fuel mass flow rate increases and the mixture coming out of the burner becomes richer, accelerating CO oxidation.

Moving to the effect of CO_2 addition, as expected, simulated EGR strongly reduces NO_x emissions, but at the same time CO levels are extremely high, almost two orders of magnitude higher than standard conditions (CO is shown with logarithmic scale). Despite the fact that all the points have the same adiabatic flame temperature, OH* images showed that the flame reactivity strongly decreases with lower oxygen content of the oxidizer. CO increase could also be linked with the downstream shift of the reaction zone, which does not allow the reaction to be completed at the probe location. Another aspect to be mentioned is the high CO_2 concentration in the oxidizer, which can participate in the combustion reaction altering the equilibrium toward the production of CO [25,26]. This last aspect is a consequence of using CO_2 dilution

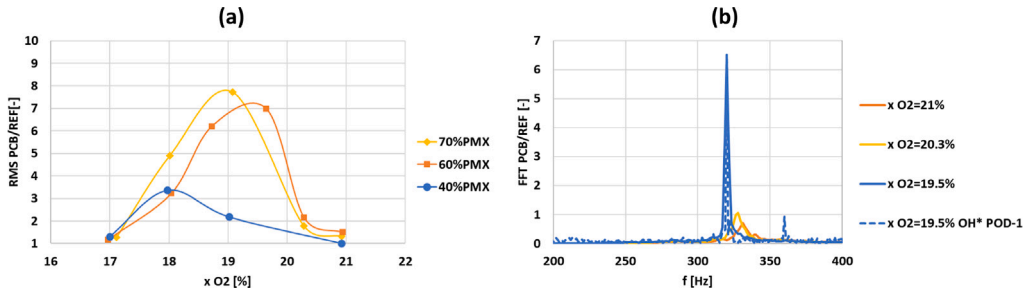

Fig. 7. Amplitude of pressure oscillation as a function of inlet oxygen molar fraction for different fuel splits (a) and frequency spectrum of pressure oscillation at 60%PMX (b).

instead of real EGR, but with the wider perspective of a comparative study the goal is not to reproduce CO emissions in absolute terms, but to be able to compare different solutions, starting from the baseline burner.

Regarding NO_x levels, simulated EGR significantly reduces the emissions, and also the effect of fuel split is lower, with NO_x still slightly growing with pilot split. In particular, with high EGR, even with very high pilot fuel fraction (low %PMX), NO_x levels are those achieved under standard conditions with high premixing. After an important drop of NO_x levels with the first level of oxygen reduction, a further decrease has a limited effect on NO_x, while CO continues to increase.

3.3. Thermoacoustic instabilities

The flame dynamic behavior is expected to change with the oxidizer composition, as enlightened by previous studies [5,7,27,28]. Being this work a preliminary screening on the main critical issues, aimed at guiding design improvement for burner operation under EGR conditions, this aspect was also investigated.

As anticipated, during the reactive tests strong tonal pressure oscillations arise when the inlet oxygen content decreases from standard air conditions. Fig. 7a reports the amplitude of pressure oscillations measured with the PCB sensor (acquisition frequency 12.8 kHz) for three different fuel splits as a function of the inlet oxygen content, with increasing EGR going from right to left. As the inlet oxygen concentration diminishes, the amplitude of these oscillations quickly grows, reaches a maximum, and eventually decreases, going back to the levels corresponding to standard air, or even lower in some cases (60%PMX). The condition where the amplitude of these pressure oscillations with CO_2 addition is the same or lower than in standard conditions (no EGR) is found to be near the flame extinction, as showed by very high CO levels and very low OH* intensity at $x_{O2} = 17\%$.

All the tested fuel splits exhibit this behavior, but the oscillation amplitude increases with the fraction of fuel supplied with the premix line. This again suggests that increasing the pilot split has a beneficial effect in terms of flame stability, and under EGR conditions the associated increase in NO_x emission, which is a limiting factor without EGR, is marginal.

Fig. 7b reports the frequency spectrum of these pressure oscillations for a fixed fuel split. The peak frequency is around 330 Hz, which corresponds to the resonance frequency of the test rig, observed also in other conditions with different burners. The peak frequency decreases with lower oxygen inlet content, and a first estimation showed that this behavior is coherent with the change in mixture composition, and therefore in thermodynamic properties as the speed of sound.

Thermoacoustic instabilities triggered by CO_2 addition in the combustion air have also been detected with OH* chemiluminescence. Fig. 8a shows instantaneous OH* images acquired under these unstable configurations, together with the time-averaged flame structure reported also for clarity (Fig. 8b). Instantaneous snapshots show that the flame is subjected to intense longitudinal fluctuations. A qualitative explanation for the non-monotonic trend of pressure oscillation with inlet oxygen level could derive from the progressive elongation and lift off of the flame with decreasing inlet oxygen level, as shown by time averaged images of Fig. 3. The coupling between heat release and pressure oscillations is altered by the variation of the flame position and length with EGR, and they result in phase only in a certain range of inlet oxygen levels, which varies with fuel split.

In order to further study the dynamic behavior and verify the presence of energetically coherent structures, POD analysis of OH* chemiluminescence images has been performed. A representative condition, the same of instantaneous OH* images of Fig. 8 (60%PMX and $x_{O2} = 19.7\%$), has been selected in order to show the main outcomes. Fig. 9a shows the energy contribution of the first 10 modes together with its cumulative (black dashed line). The first mode alone contains almost half of the total energy, which indicates the presence of coherent structures with an important energy contribution. The frequency spectrum of this POD first mode corresponds to the dashed line in Fig. 7, and, as expected, it perfectly overlaps with the pressure oscillation peak detected with the PCB (OH* spectrum amplitude is showed in arbitrary units). A second peak at higher frequency is also present but with a significantly lower amplitude.

The spatial distribution of the first POD mode is reported in Fig. 9b, and it shows very defined structures. The two spots with high positive values at the flame base near the liner walls indicate that local OH* intensity (and therefore heat release) is oscillating with energy comparable to that of the main central zone (high negative values) but in counter-phase. Recalling also the time averaged flame structure of Fig. 8b to locate the pilot fuel jets, POD first mode structure suggests that these thermoacoustic instabilities are strongly affected by the interaction between pilot flames and the central reaction zone of the premixed fuel.

The main outcome of these results is that pilot fuel jets assume an even more crucial role for flame stability when the burner is operated under EGR-like conditions. The optimization of the burner design can benefit from less stringent limitations for NO_x emissions, which are already lowered by EGR. Therefore, higher pilot fuel splits can be exploited to help the flame stabilization, and pilot flames configuration becomes a key parameter. With this perspective, unconventional pilot flames could be also employed, such as local injections of hydrogen to increase the mixture reactivity in strategical positions, in reduced amount so as not to decrease the CO_2 content in the exhaust. The study of this aspect is the goal of the next experimental campaign, which just begun and is showing interesting results so far.

4. Conclusions

In the present work the experimental characterization of an industrial burner with reduced inlet oxygen content has been presented. The purpose of the study is to explore the behavior of the burner under EGR-like conditions in order to identify driving parameters for design optimization aimed at expanding the burner stability limits.

The burner was fueled with natural gas and operated at ambient pressure in an optical single sector test rig. EGR has been reproduced by diluting the combustion air with CO_2, and fuel split between pilot and premixed line has been varied.

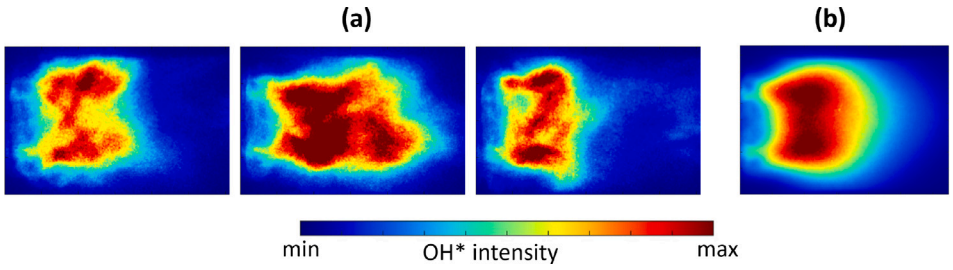

Fig. 8. Instantaneous (a) and time averaged (b) OH* images for 60%PMX and x_{O2} = 19.7% acquired at 1000 Hz.

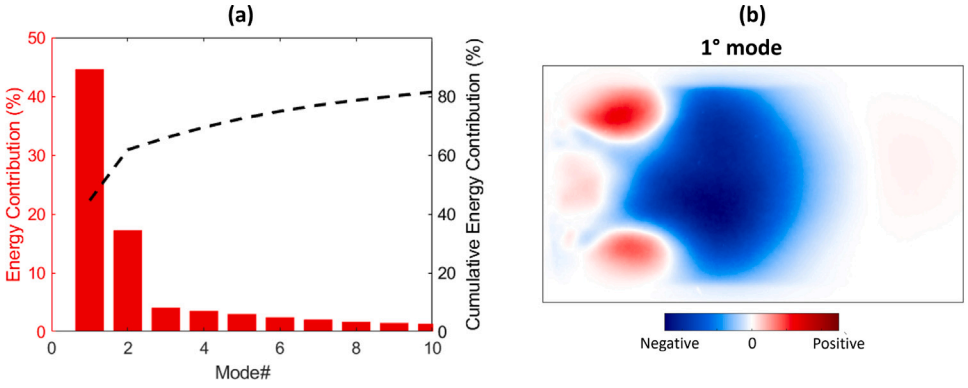

Fig. 9. Energy contribution of the first ten POD modes (a) and spatial distribution of POD Mode 1 extracted from OH* chemiluminescence images for 60%PMX and x_{O2} = 19.7%.

OH* chemiluminescence showed very different flame structures varying the fuel split and oxidizer composition. The main reaction zone corresponds to the diffusive pilot flames, which are responsible for flame stabilization even when the fuel fraction injected with the pilot line is limited. As the oxygen content in the combustion air decreases the reaction zone becomes widespread, OH* intensity drops and flame length significantly increases especially for higher premixed cases.

Emission measurements revealed very high CO levels under EGR-like conditions, progressively increasing with CO_2 addition. CO rise can be correlated to both air vitiation and the reduced residence time of the rig, as the flame significantly elongates in such conditions. NO_x emissions, on the other hand, benefit from the lower oxygen content, and the dependency on fuel split, which is very strong in standard conditions, becomes marginal.

Thermoacoustic instabilities have been observed, triggered by CO_2 addition in the oxidizer until it exceeds a certain threshold level. POD analysis of high speed OH* chemiluminescence acquired at these unstable conditions revealed the presence of coherent structures born from the interaction between pilot and premixed reaction zones. The oscillations amplitude increases with the premix fuel split, suggesting the adoption of lower premixing levels to improve flame stability, which in oxygen depleted conditions can be achieved without incurring in NO_x increase.

At the moment the outbreak of thermoacoustic instabilities and high CO emissions are reducing the burner operating window in EGR-like conditions, but the collected results provide important insights to guide improvements in the burner performance, as the crucial role of pilot fuel injection mode. Additionally, the present results will also be used to validate numerical models for CFD simulations of the combustion process under these unconventional conditions, for which only few experimental data are available.

CRediT authorship contribution statement

S. Galeotti: Data curation, Investigation, Writing – original draft, Writing – review & editing. **A. Picchi:** Investigation, Supervision, Writing – review & editing. **R. Becchi:** Investigation, Supervision. **R. Meloni:** Supervision. **G. Babazzi:** Supervision. **C. Romano:** Supervision. **A. Andreini:** Conceptualization, Methodology, Project administration, Supervision, Writing – review & editing.

Declaration of competing interest

The authors declare the following financial interests/personal relationships which may be considered as potential competing interests: Antonio Andreini reports financial support was provided by Horizon Europe. If there are other authors, they declare that they have no known competing financial interests or personal relationships that could have appeared to influence the work reported in this paper.

Data availability

The data that has been used is confidential.

Acknowledgments

This project has received funding from the European Union's Horizon Europe research and Innovation programme under Grant Agreement No 101069665

Funded by the European Union

Funded by the European Union. Views and opinions expressed are however those of the author(s) only and do not necessarily reflect those of the European Union. Neither the European Union nor the granting authority can be held responsible for them.

References

[1] IEA, World Energy Outlook 2022, Technical Report, IEA, Paris, France, 2022, License: CC BY 4.0 (report).

[2] H. Li, M. Ditaranto, D. Berstad, Technologies for increasing CO2 concentration in exhaust gas from natural gas-fired power production with post-combustion, amine-based CO2 capture, Energy 36 (2) (2011) 1124–1133, http://dx.doi.org/10.1016/j.energy.2010.11.037.

[3] D. Burnes, P. Saxena, P. Dunn, Study of using exhaust gas recirculation on a gas turbine for carbon capture, in: Volume 5: Controls, Diagnostics, and Instrumentation; Cycle Innovations; Cycle Innovations: Energy Storage, in: Turbo Expo: Power for Land, Sea, and Air, 2020, p. V005T06A034. http://dx.doi.org/10.1115/GT2020-16080.

[4] T. Lieuwen, M. Chang, A. Amato, Stationary gas turbine combustion: Technology needs and policy considerations, Combust. Flame 160 (8) (2013) 1311–1314, http://dx.doi.org/10.1016/J.COMBUSTFLAME.2013.05.001.

[5] A.M. ElKady, A. Evulet, A. Brand, T.P. Ursin, A. Lynghjem, Exhaust gas recirculation in DLN F-class gas turbines for post-combustion CO2 capture, in: Volume 3: Combustion, Fuels and Emissions, Parts A and B, in: Turbo Expo: Power for Land, Sea, and Air, 2008, pp. 847–854, http://dx.doi.org/10.1115/GT2008-51152.

[6] G. Babazzi, N. Giannini, R. Meloni, P.C. Nassini, G. Lemmi, A. Andreini, On the impact of the EGR on to the operability of a heavy-duty GT combustor: a CFD investigation, in: Proc. of the 11th European Combustion Meeting, Rouen, France, 2023.

[7] J. Rodriguez Camacho, M. Akiki, J. Blust, J. O'Connor, Effect of inert species on the static and dynamic stability of a piloted, swirl-stabilized flame, J. Eng. Gas Turb. Power 146 (6) (2024) 061021, http://dx.doi.org/10.1115/1.4064048.

[8] T. Wilberforce, A. Olabi, E.T. Sayed, K. Elsaid, M.A. Abdelkareem, Progress in carbon capture technologies, Sci. Total Environ. 761 (2021) 143203, http://dx.doi.org/10.1016/j.scitotenv.2020.143203.

[9] M. Cerutti, N. Giannini, G. Ceccherini, R. Meloni, E. Matoni, C. Romano, G. Riccio, Dry low NOx emissions operability enhancement of a heavy-duty gas turbine by means of fuel burner design development and testing, in: Volume 4B: Combustion, Fuels, and Emissions, in: Turbo Expo: Power for Land, Sea, and Air, 2018, p. V04BT04A029. http://dx.doi.org/10.1115/GT2018-76587.

[10] A. Andreini, B. Facchini, A. Innocenti, M. Cerutti, Numerical analysis of a low NOx partially premixed burner for industrial gas turbine applications, Energy Procedia 45 (2014) 1382–1391, http://dx.doi.org/10.1016/j.egypro.2014.01.145.

[11] A. Innocenti, A. Andreini, A. Giusti, B. Facchini, M. Cerutti, G. Ceccherini, G. Riccio, Numerical investigations of NOx emissions of a partially premixed burner for natural gas operations in industrial gas turbine, in: Volume 4B: Combustion, Fuels and Emissions, in: Turbo Expo: Power for Land, Sea, and Air, 2014, p. V04BT04A045. http://dx.doi.org/10.1115/GT2014-26906.

[12] A. Innocenti, A. Andreini, B. Facchini, M. Cerutti, G. Ceccherini, G. Riccio, Design improvement survey for NOx emissions reduction of a heavy-duty gas turbine partially premixed fuel nozzle operating with natural gas: Numerical assessment, J. Eng. Gas Turb. Power 138 (1) (2015) 011501, http://dx.doi.org/10.1115/1.4031144.

[13] M. Cerutti, M. Roma, A. Picchi, R. Becchi, B. Facchini, Improving emission and blow-out characteristics of novel natural gas low NOx burners for heavy duty gas turbine, in: Volume 4B: Combustion, Fuels, and Emissions, in: Turbo Expo: Power for Land, Sea, and Air, 2019, p. V04BT04A015. http://dx.doi.org/10.1115/GT2019-91235.

[14] M. Cerutti, G. Riccio, A. Andreini, R. Becchi, B. Facchini, A. Picchi, Experimental and numerical investigations of novel natural gas low NOx burners for heavy duty gas turbine, in: Volume 4B: Combustion, Fuels, and Emissions, in: Turbo Expo: Power for Land, Sea, and Air, 2018, p. V04BT04A031. http://dx.doi.org/10.1115/GT2018-76670.

[15] S. Kline, F.A. McClintock, Describing uncertainties in single-sample experiments, Mech. Eng. 75 (1953) 3–8.

[16] G. Babazzi, Experimental Investigation of Novel Gas Turbine Combustor Concepts Operating with CO2 Vitiated Air (Ph.D. thesis), Universià degli Studi di Firenze, 2022.

[17] L. Montgomery Smith, D.R. Keefer, S.I. Sudharsanan, Abel inversion using transform techniques, J. Quant. Spectrosc. Radiat. Transfer 39 (5) (1988) 367–373, http://dx.doi.org/10.1016/0022-4073(88)90101-X.

[18] L. Sirovich, Turbulence and the dynamics of coherent structures. I - Coherent structures. II - symmetries and transformations. III - dynamics and scaling, Quart. Appl. Math. - QUART APPL MATH 45 (1987) http://dx.doi.org/10.1090/qam/910463.

[19] A.-M. Kypraiou, A. Dowling, E. Mastorakos, N. Karimi, Proper orthogonal decomposition analysis of a turbulent swirling self-excited premixed flame, in: 53rd AIAA Aerospace Sciences Meeting, 2015, http://dx.doi.org/10.2514/6.2015-0425.

[20] J. Lumley, The structure of inhomogeneous turbulent flows, in: Atmospheric Turbulence and Radio Wave Propagation, 1967, pp. 166–177.

[21] F. Guethe, D. Guyot, G. Singla, N. Noiray, B. Schuermans, Chemiluminescence as diagnostic tool in the development of gas turbines, Appl. Phys. B 107 (3) (2012) 619–636, http://dx.doi.org/10.1007/s00340-012-4984-y.

[22] J. Natarajan, T. Lieuwen, J. Seitzman, Laminar flame speeds of H2/CO mixtures: Effect of CO2 dilution, preheat temperature, and pressure, Combust. Flame 151 (2007) 104–119, http://dx.doi.org/10.1016/j.combustflame.2007.05.003.

[23] B. Galmiche, F. Halter, F. Foucher, P. Dagaut, Effects of dilution on laminar burning velocity of premixed methane/air flames, Energy Fuels 25 (3) (2011) 948–954, http://dx.doi.org/10.1021/ef101482d.

[24] G. Babazzi, S. Galeotti, A. Picchi, R. Becchi, M. Cerutti, A. Andreini, Combustion diagnostics and emissions measurements of a novel low NOx burner for industrial gas turbine operated with CO2 diluted methane/air mixtures, J. Eng. Gas Turb. Power 146 (7) (2024) 071007, http://dx.doi.org/10.1115/1.4064266.

[25] F. Liu, H. Guo, G.J. Smallwood, The chemical effect of CO2 replacement of N2 in air on the burning velocity of CH4 and H2 premixed flames, Combust. Flame 133 (4) (2003) 495–497, http://dx.doi.org/10.1016/S0010-2180(03)00019-1.

[26] M. Lubrano Lavadera, P. Sabia, G. Sorrentino, R. Ragucci, M. de Joannon, Experimental study of the effect of CO2 on propane oxidation in a Jet Stirred Flow Reactor, Fuel 184 (2016) 876–888, http://dx.doi.org/10.1016/j.fuel.2016.06.046.

[27] D. Ferguson, J.A. Ranalli, P. Strakey, Influence of Exhaust Gas Recirculation on Combustion Instabilities in CH4 and H2/CH4 Fuel Mixtures, in: Volume 2: Combustion, Fuels and Emissions, Parts A and B, in: Turbo Expo: Power for Land, Sea, and Air, 2010, pp. 1259–1267, http://dx.doi.org/10.1115/GT2010-23642.

[28] A.T. Evulet, A.M. ELKady, A.R. Branda, D. Chinn, On the performance and operability of GE's dry low NOx combustors utilizing exhaust gas recirculation for post-combustion carbon capture, Energy Procedia 1 (2009) 3809–3816.